LIMNOLOGY and OCEANOGRAPHY: METHODS

Limnol. Oceanogr.: Methods 10, 2012, 752–766

Using cavity ringdown spectroscopy for continuous monitoring of $\delta^{13}C(CO_2)$ and fCO_2 in the surface ocean

*M. Becker[1,2], N. Andersen[3], B. Fiedler[2], P. Fietzek[2,4], A. Körtzinger[2], T. Steinhoff[2], and G. Friedrichs[1]**

[1]Institute of Physical Chemistry, Christian-Albrecht University, Kiel, Germany
[2]GEOMAR, Helmholtz Centre for Ocean Research, Kiel, Germany
[3]Leibniz-Laboratory for Radiometric Dating and Stable Isotope Research, Kiel, Germany
[4]CONTROS Systems and Solutions GmbH, Kiel, Germany

Abstract

The role of the global surface ocean as a source and sink for atmospheric carbon dioxide and the flux strengths between the ocean and the atmosphere can be quantified by measuring the fugacity of CO_2 (fCO_2) as well as the dissolved inorganic carbon (DIC) concentration and its isotopic composition in surface seawater. In this work, the potential of continuous wave cavity ringdown spectroscopy (*cw*-CRDS) for autonomous underway measurements of fCO_2 and the stable carbon isotope ratio of DIC [$\delta^{13}C(DIC)$] is explored. For the first time, by using a conventional air-sea equilibrator setup, both quantities were continuously and simultaneously recorded during a field deployment on two research cruises following meridional transects across the Atlantic Ocean (Bremerhaven, Germany–Punta Arenas, Chile). Data are compared against reference measurements by an established underway CO_2 monitoring system and isotope ratio mass spectrometric analysis of individual water samples. Agreement within $\Delta fCO_2 = 0.35$ µatm for atmospheric and $\Delta fCO_2 = 2.5$ µatm and $\Delta\delta^{13}C(DIC) = 0.33$‰ for seawater measurements have been achieved. Whereas "calibration-free" fCO_2 monitoring is feasible, the measurement of accurate isotope ratios relies on running reference standards on a daily basis. Overall, the installed CRDS/equilibrator system was shown to be capable of reliable online monitoring of fCO_2, equilibrium $\delta^{13}C(CO_2)$, $\delta^{13}C(DIC)$, and pO_2 aboard moving research vessels, thus making possible corresponding measurements with high spatial and temporal resolution.

One of the major drivers of climate change is the accumulation of carbon dioxide in the atmosphere. So far, approximately 48% of the anthropogenically emitted CO_2 have been dissolved in the oceans (Sabine et al. 2004). To determine more precisely the magnitude of the net ocean sink, the gas fluxes between atmosphere and surface ocean have to be determined (Keeling et al. 2005). Besides the difference of atmospheric and oceanic CO_2 fugacity (ΔfCO_2), the isotope signature of the carbon reservoirs can be used to estimate the corresponding fluxes.

*Corresponding author: E-mail: friedrichs@phc.uni-kiel.de; Institut für Physikalische Chemie, Christian-Albrechts-Universität zu Kiel, Olshausenstr. 40, 24098 Kiel, Germany.

Acknowledgments.

We would like to acknowledge Julia Bock for her initial work on this method and the preparation of the instrument for the first cruise. Many thanks go to the captain and crew of R/V *Polarstern*. This study was supported by the German Science Foundation (DFG-EC80) in the framework of the cluster of excellence "The Future Ocean" and through the project OCEANET of the WGL Leibniz Association.

DOI 10.4319/lom.2012.10.752

The stable isotope abundance of carbon is reported relative to the reference standard V-PDB (Vienna-PeeDee Belemnite) in terms of $\delta^{13}C$ in ‰:

$$\delta^{13}C = \left(\frac{\left({}^{13}C/{}^{12}C \right)_{measured}}{\left({}^{13}C/{}^{12}C \right)_{V\text{-}PDB}} - 1 \right) \times 1000 \quad (1)$$

In general, isotope measurements are known as useful tracers to elucidate mass flows between different reservoirs. Without the need for additional measuring parameters, they depict seasonal and interannual variability within the carbonate system as well as fluxes between different carbon sources that are mediated by biological uptake and release, mixing, and gas exchange (e.g., Quay et al. 2007, 2009). The utility of isotope ratio information for understanding surface ocean carbon dynamics, however, is limited by the scarce number of available $\delta^{13}C$ measurements for oceanic CO_2 or dissolved inorganic carbon (DIC). Whereas fCO_2 is commonly determined using continuous and autonomous underway techniques, single point $\delta^{13}C$ values are typically measured by isotope ratio mass spectrometry (IRMS). With an accuracy of better than 0.05‰ (de Groot 2004) in measuring the isotope ratio in

gaseous CO_2, IRMS meets the high accuracy demands to measure the observed small changes in the ‰-range. So far, the required time-consuming and expensive sample handling including collection, shipment, and processing precludes IRMS based $\delta^{13}C$ measurements in underway mode. Moreover, to achieve the required accuracy, very frequent calibration of the mass spectrometer is necessary (Ghosh and Brand 2003). Altogether, this leads to a strong limitation of the sampling rate resulting in low spatial and temporal coverage of field data. For example, until the year 2003 the entire $\delta^{13}C$(DIC) data set for the global ocean consisted of only about 25000 data points (Quay et al. 2003) as opposed to approx. 5.2 million fCO_2 measurements collected between 1957 and 2010 listed in the Lamont-Doherty Earth Observatory (LDEO) database (Takahashi et al. 2011).

Extensive efforts have been undertaken to overcome these limitations by measuring isotope ratios using optical spectroscopy. As isotope substitution causes spectral shifts in the rovibrational transitions of a molecule, the concentrations of each isotopologue can easily be determined by high resolution absorption measurements. Supposing that the absorption cross section is known, an important advantage of absorption-based methods is that calibration is (in principle) not necessary. Following first laser-based optogalvanic measurements performed by Murnick and Peer (1994), many different spectroscopic methods have been tested. Examples are tunable diode laser absorption spectroscopy (TDLAS) (Bergamaschi et al. 1994), nondispersive infrared spectroscopy (NDIR) (Haisch et al. 1994; Jäger et al. 2005), Fourier transform infrared spectroscopy (FTIR) (Mohn et al. 2007), and cavity enhanced or cavity ringdown methods (Crosson et al. 2002; Jost et al. 2006; Wahl et al. 2006).

For ship deployment, the spectrometer needs to withstand vibrations caused by ship operation. For continuous measurements, for example on a voluntary observing ship (VOS), autonomous operation must be possible as well. Durable NDIR detectors have proven to be suitable for fCO_2 measurements in surface water in such applications, [e.g., Körtzinger et al. (2000)]. However, their sensitivity and spectral resolution is not sufficient for isotope ratio measurements. Even for fCO_2 monitoring, regular calibration with several different gas standards is needed to assure the desired accuracy of approx. 1 µatm. Improvements can be expected by using sensitive cavity ringdown spectroscopy (CRDS) instruments. During a CRDS experiment, a narrow-bandwidth laser beam encounters multiple reflections within a resonant optical cavity. This cavity is filled with the test gas, hence it represents the sample cell. As will be explained in more detail below, CRDS is immune against laser intensity fluctuations, which often limit the precision of other types of absorption experiments. This combination of long effective absorption pathlength, immunity to light intensity noise, as well as the possibility to measure spectra in high spectral resolution makes CRDS an ultrasensitive detection method for all sorts of stable and transient molecules, including CO_2 (Friedrichs 2008; Kerstel and Gianfrani 2008). Recently, easy-to-handle and robust isotope ratio CRDS as well as cavity-enhanced absorption spectroscopy (CEAS) instruments entered the market and have been successfully used to perform isotope selective field measurements on land (Graham et al. 2010; Gupta et al. 2009; Krevor et al. 2010; McAlexander et al. 2011) and in coral reefs (Bass et al. 2012).

In a preceding article, we have provided a thorough characterization of such a CRDS instrument by determination of its precision and accuracy. Moreover a first coupling with an air-water equilibrator has been accomplished (Friedrichs et al. 2010). In the present work, a field test of the same CRDS analyzer was performed aboard the German research vessel Polarstern. To measure surface water fCO_2, stable carbon isotope ratios, and oxygen concentrations, the instrument was coupled to an underway air-seawater equilibration system. The performance of the setup was tested during two meridional research cruises throughout the Atlantic Ocean between Punta Arenas, Chile, and Bremerhaven, Germany (Fig. 1). A detailed assessment and a comparison with reference data measured by common methods are presented here.

Note that throughout this manuscript when referring to seawater properties $\delta^{13}C(CO_2)$ denotes the $\delta^{13}C(CO_2)$ of CO_2 in air, which is in chemical equilibrium with the sampled seawater. It does not stand for the ^{13}C isotopic ratio of the individual CO_2 species in the seawater DIC pool.

Materials and procedure

Cavity ringdown spectroscopy

Cavity ringdown spectroscopy (CRDS) is a highly sensitive spectroscopic technique. In contrast to most other absorption schemes, in CRDS the absorption is measured in the time instead of the intensity domain. A narrow bandwidth laser beam is coupled into a resonant optical cavity consisting of two or more highly reflective mirrors. Typical reflectivities are around 99.99% in the used wavelength region. Within the cavity, the laser light is reflected back and forth resulting in long effective pathlengths of up to several kilometers. In continuous wave CRDS (*cw*-CRDS) using laser diodes as the light source, the narrow bandwidth detection light needs to be coupled resonantly into the cavity by piezo-tuning one of the mirrors. With a resonant cavity, light intensity starts to build up in the cavity, and after a preset intensity level is reached, the laser is shut-off quickly, e.g., by an acousto-optical modulator (Romanini et al. 1997). Subsequently, a small part of the intensity is lost upon each roundtrip of the light and is detected by a photodetector placed behind the rear mirror. The decay constant of the resulting mono-exponential intensity-time profile, the so-called ringdown signal, reflects the quality of the ringdown cavity. Typical ringdown times are on the order of tens of microseconds corresponding to effective absorption pathlengths of several kilometers. In presence of an absorber within the cavity and in consequence of the additional intensity loss caused by absorption, the observed decay

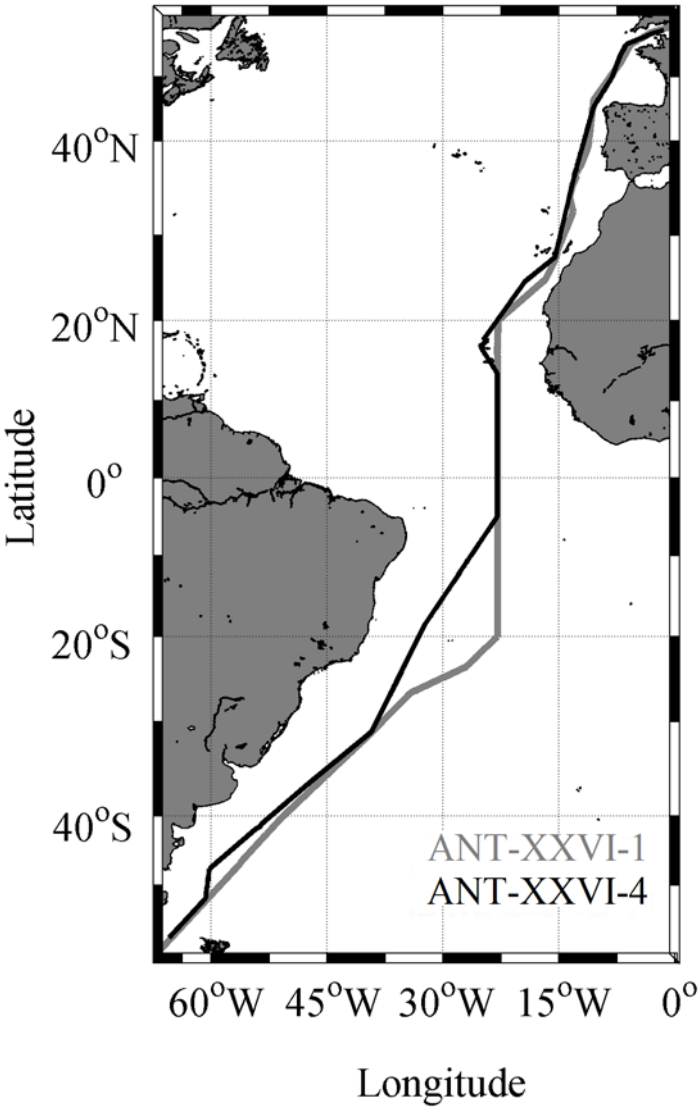

Fig. 1. Cruise tracks of ANT-XXVI/1 (gray line) and ANT-XXVI/4 (black line).

time becomes shorter with increasing absorber concentration. The absorption coefficient $\alpha(\nu)$ at laser frequency ν can be directly determined from the difference of two time constants

$$\alpha(\nu) = \frac{1}{c}\left(\frac{1}{\tau} - \frac{1}{\tau_0}\right) \quad (2)$$

with τ_0 referring to the decay time of the empty cavity and τ referring to the decay time of the cavity with absorber present; c is the speed of light. Smallest detectable absorptions are typically around $\alpha_{min} = 10^{-9}$ cm^{-1} (Mazurenka et al. 2005). For acquisition of absorption line profiles, the laser frequency is scanned over the absorption feature of interest. The absorption line strengths can be directly determined from the measured spectrum and the $\delta^{13}C(CO_2)$ value is deduced from the ratio of the absorption of two separate $^{12}CO_2$ and $^{13}CO_2$ spectral lines.

***cw*-CRDS analyzer**

A commercial *cw*-CRDS analyzer (EnviroSense 2050, Picarro) was used to measure $^{12}CO_2$, $^{13}CO_2$, and water vapor concentrations. A diode laser with an emission maximum around 1600 nm was coupled into a piezo-tuned 3-mirror-cavity. The sample gas was pumped through the cavity by a membrane pump with a flow of about 20 sccm (standard cm^3) at a pressure of 186.6 mbar and a temperature of 45.0°C. The species were detected on rovibrational absorption lines corresponding to the 30013←00001 transition of the R(36)-line of $^{12}CO_2$ at 6251.76 cm^{-1}, the 30012←00001 transition of the R(12)-line of $^{13}CO_2$ at 6251.32 cm^{-1}, and the 040,5,5,0←000,6,6,1 transition of H_2O at 6250.42 cm^{-1} (Mikhailenko et al. 2008; Perevalov et al. 2008a, 2008b). The absorption profiles were sampled with a scan increment of 0.02 cm^{-1} using a patented etalon-based wavelength monitor. Raw data points were created every 8–12 s based on hundreds of ringdown events. Artifacts such as irregular appearing spikes in the $^{13}CO_2$-measurements and switching spikes due to pressure variations caused by changing the gas flow were cut out of all data traces before data analysis. The acquired spectra were fitted with a multi-order fitting routine based on Galatry line profiles with line shape parameters valid for ambient air. Besides Doppler and pressure broadening, Galatry line profiles take into account the collisional Dicke narrowing effect (Galatry 1961). The three fitting parameters were the Doppler width, the collisional broadening parameter y, and the narrowing parameter z. To assure stable fitting results, the ratio y/z was kept at a fixed value of 0.3215. For the determination of the mole fractions of $^{12}CO_2$, $^{13}CO_2$, and water vapor, peak heights of fitted Galatry lines were used instead of integrated absorption. This reduced possible errors arising from residual baseline fitting issues, but also introduced a gas matrix dependence due to subtle pressure line broadening effects. For example, in our previous work (Friedrichs et al. 2010), it was shown that a 1% oxygen change in the gas matrix from the ambient air oxygen content corresponds to a systematic offset of the measured $\delta^{13}C(CO_2)$ value of 0.5‰. A further check of the validity of a spectroscopically based correction procedure put forward in that previous article is one of the objectives of this work.

The CRDS xCO_2 was calibrated during pre-cruise measurements with an accuracy of ± 0.5 ppmv. Note that the standard measurements during the cruise (see below) were not included in the fCO_2 calculation. The isotopic compositions of the used reference gas standards were characterized by IRMS with an accuracy of ± 0.05‰. The accuracy of the isotope ratio measurements by CRDS was determined by Allan deviation analysis (Friedrichs et al. 2010). Briefly, for an ideal analyzer with only statistical noise components, the precision of the measurements should improve with the square root of the number of averaged measurements. In a real experiment, however, this improvement is limited by long-term drift components. For our instrument, the optimum averaging time was

found to be on the order of τ_{opt} = 150 min resulting in a precision of $\Delta[\delta^{13}C(CO_2)]$ = ± 0.07‰. An attainable accuracy including the long-term drift components was estimated to be ± 0.15‰. In this work, to improve the time response, a moving average over τ = 60 min has been calculated from the original field data corresponding to a precision of $\Delta(\delta^{13}C(CO_2))$ = ± 0.1‰ and an attainable accuracy of ± 0.25‰.

Setup and procedure aboard R/V Polarstern

Following a first performance test during the cruise ANT-XXVI/1 (from 50°N to 50°S) in October/November 2009, $\delta^{13}C(CO_2)$ and fCO_2 in surface seawater were measured continuously in underway-mode during the cruise ANT-XXVI/4 (from 50°S to 50°N) in April/May 2010. The cruise tracks are shown in Fig. 1 and the schematic setup of the equilibration system in Fig. 2. The CRDS was coupled to a commercial sprayhead equilibration system (Model 8050, General Oceanics), in the following referred to as GO-System, which is described in detail in Pierrot et al. (2009). Seawater flowed continuously with a rate of 3 L min^{-1} through the equilibrator and formed a circular spray. After equilibration of the overlying gas phase to the continuous seawater flow, the equilibrated gas phase was dried by a thermoelectrically cooled condenser at 6°C and afterward by a Permapure Nafion dryer resulting in < 0.2% H_2O by volume before entering the analyzer. The continuous flow of the sample gas was set to 100 sccm with 20 sccm flowing through the CRDS analyzer in a bypass configuration. Using a multiposition valve assembly, it was possible to measure either the gas from the equilibrator, a reference gas standard, or marine air. The equilibrator gas was recirculated in a closed loop to the equilibrator, all other gases were rejected after measurement. Internal leaking of the CRDS pumping unit, which has been reported for the used analyzer series, had been resolved by thorough sealing of the fittings on the gas tubing. Equilibrator temperature and pressure were measured directly. Each day, a reference gas standard with $\delta^{13}C(CO_2)$ = (10.42 ± 0.05) ‰ and xCO_2 = (350 ± 3) ppmv was measured for 3 h and marine air for 1–2 h. Sea surface temperature and salinity were measured by a thermosalinograph near the water intake at the keel and atmospheric temperature and pressure were recorded by the weather station at the top of the ship. To assess the quality of the CRDS data, reference measurements were performed by conventional methods in parallel. The carbon dioxide fugacity was measured in underway-mode by an NDIR detector (LI-7000 CO_2/H_2O Analyzer, LiCOR) coupled to a separate, nearly identical GO-equilibration system operated on the same water supply. The NDIR detector was calibrated by the use of four working standards that had been carefully calibrated against NOAA standards (accuracy 0.1 ppmv) before the cruise. A linear regression was used to generate a calibration curve as reported in Pierrot et al. (2009). This resulted in an accuracy of 2 µatm in measuring seawater fCO_2 and 0.1 µatm for atmospheric measurements. The CO_2 data were processed after the best practice guidelines of the U.S. Department of Energy (DOE) (Dickson et al. 2007).

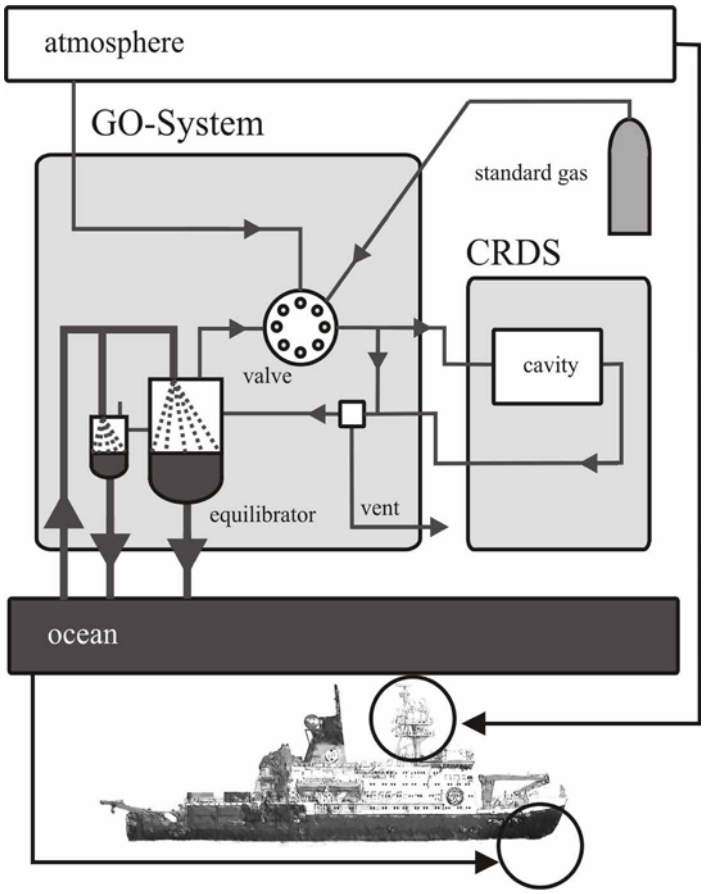

Fig. 2. Schematic setup of the water supply, equilibration system, and gas pathways aboard R/V Polarstern.

As $\delta^{13}C(CO_2)$ reference, discrete samples of 100 mL surface water were collected, poisoned with 50 µL saturated mercuric chloride solution and analyzed by IRMS at the Leibniz Laboratory for Radiometric Dating and Stable Isotope Research in Kiel. On the basis of duplicates, the uncertainty of the mass spectrometric analyses was estimated to be $\Delta[\delta^{13}C(DIC)]$ = ± 0.075‰. Finally, the oxygen concentration was measured by an optode sensor (Model 3830, Aanderaa) in a flow-through box with an accuracy of about 8 µmol kg^{-1} (≈0.008 atm). The optode was calibrated only once (at 25°C) against Winkler oxygen data. Therefore, as it is known that optodes often show a temperature-dependent performance, the measurements in cold water at higher latitudes are less reliable and need to be handled with care. As for fCO_2, the reported underway pO_2 data have been converted to atmospheric pressure conditions to facilitate a direct comparison with the equilibrator measurements. For this purpose, the total gas pressure of dissolved gases was measured with a gas tension device (GTD sensor).

***f*CO_2 calculations**

To process the CRDS data for fCO_2, the concentrations of both isotopologues were summed up, and the data were cor-

rected to dry air values by using the measured water vapor content. Moreover, as will be outlined below, a gas matrix correction was applied by using the measured oxygen mole fraction (optode data) as a single input parameter for calculating the gas matrix composition. Finally, the derived dry mole fractions of CO_2 were converted to fCO_2 at ambient pressure and 100% water vapor saturation according to Dickson et al. (2007).

$\delta^{13}C(CO_2)$ calculations

The isotope ratio is calculated from the concentrations of each isotopologue by the instrument's software using a calibration polynomial. A gas matrix correction was applied based on the simultaneously detected oxygen concentrations from the optode according to $\Delta(\delta^{13}C(CO_2)) = \sum x_i \phi_i$. Here, ϕ_i represents the gas matrix offset factor of component i as listed in Table 1.

For example, the value of $\phi(O_2)$ = –38.7‰ corresponds to a –38.7‰ underestimation in the $\delta^{13}C(CO_2)$ value measured by the instrument when replacing air by pure oxygen (Friedrichs et al. 2010). According to a recent manufacturer service release, the used $^{13}CO_2$ absorption line for CRDS analysis is also affected by an interfering weak CH_4 absorption line. This interference causes a significant bias in the $\delta^{13}C(CO_2)$ value for samples with CH_4 content different from the CH_4 contents in the reference gas standard. A recommended, first order correction of this cross sensitivity is based on the equation

$$\delta^{13}C(CO_2)_{real} = \delta^{13}C(CO_2)_{reported} - A \times \frac{xCH_4}{xCO_2} \quad (3)$$

An approximate correction factor of A ≈ 200 has been reported by the manufacturer. It is expected to depend slightly on the water concentration and may somewhat vary from analyzer to analyzer. The magnitude of this correction amounts to ≈ 0.95‰ for a CH_4 mole fraction of 1.8 ppmv and an xCO_2 of 380 ppmv in the measured sample gas.

To correct for a remaining systematic error because of an oscillating drift of the spectrometer, a reference gas standard was measured daily and interpolated values were deduced from a fitted spline as shown below.

For comparison with the IRMS data, the CRDS isotope ratio data had to be converted to the isotope ratio of DIC. The corresponding isotope fractionation, $\varepsilon_{DIC-CO_2(g)}$, depends on temperature, salinity and the speciation of the carbonate system. Fractionation factors measured by Zhang et al. (1995) in seawater (North Pacific, salinity not specified) were used for data processing according to Eq. 4,

$$\frac{\varepsilon_{(DIC-CO_2(g))}}{‰} = 10.53 - 0.107 \times \frac{T}{°C} + 0.014 \times f_{CO_3^{2-}} \times \frac{T}{°C} \quad (4)$$

which is valid for 5°C < T < 25°C, 0.05 < $f_{CO_3^{2-}}$ < 0.20, and 7.5 < pH < 8.5. For T, we used sea surface temperature. The carbonate fraction ($f_{CO_3^{2-}} = [CO_3^{2-}]/[DIC]$) was calculated using the corresponding fCO_2 data and a total alkalinity (TA), which was estimated from a TA-salinity correlation ($TA/(\mu mol\ kg^{-1}) = (54 \pm 1) \times S + (420 \pm 40)$) based on discrete TA samples, which were collected during the cruise ANT-XXIV/4. All calculations were performed using the inorganic carbon model CO2SYS (van Heuven et al. 2009) with the dissociation constants of Mehrbach et al. (1973) as refitted by Dickson and Millero (1987). As neither underway measurements nor discrete sampling of silicate and phosphate have been performed, the minor contribution of these nutrients to TA was neglected.

***p*O_2 calculations and oxygen experiment**

Assuming a fixed Ar/N_2 ratio in the sampled gas, which was set to the value of ambient air (r = 0.01/0.781), it is possible to calculate the O_2 content from the Galatry line shape parameter y (Friedrichs et al. 2010) as follows:

$$x\,O_2 = \frac{(1-r)\left(y - x\,H_2O \times y^{o}_{H_2O}\right) - (1 - x\,H_2O)\left(ry^{o}_{Ar} + ry^{o}_{N_2}\right)}{(1-r)ry^{o}_{O_2} - ry^{o}_{Ar} - ry^{o}_{N_2}} \quad (5)$$

Here, the y_i represent the y-values that have been determined by fitting the observed absorption line shapes using the respective pure gases. Values used can be found in Table 1. In this way, although not directly measuring O_2 absorption, the instrument can be used to deduce the gas phase oxygen mole fraction, which is needed to correct for the gas matrix effect outlined above. The precision of the determined y_i values was found to be ± 0.0015 corresponding to an uncertainty of ± 0.5% in the mole fraction of oxygen. Using the mole fraction of O_2 from Eq. 5, pO_2 was calculated according to Eq. 6.

$$pO_2 \approx xO_2 \times \left(p_{equ} - pH_2O\right) \quad (6)$$

Here, p_{equ} and pH_2O are the measured total pressure and the partial pressure of H_2O inside the equilibrator, respectively.

To further verify the gas matrix correction procedure, batch experiments were performed with water samples featuring large variations in the oxygen concentration. These experiments were conducted off the coast of West Africa, where a pronounced oxygen minimum zone can be found at a water depth of about 400 m (Stramma et al. 2008). From several depths between the surface and 400 m, 80 L seawater were sampled with a CTD rosette and pumped directly from the Niskin samplers through the equilibrator using a peristaltic pump at a flow rate of 2.5 L min^{-1}. In this way, each batch

Table 1. Gas matrix offset factors ϕ_i and Galatry line shape collisional broadening parameters y_i for the gases H_2O, N_2, O_2, Ar, He, and air; adopted from Friedrichs et al. (2010).

	H_2O	Ar	N_2	O_2	He	air
ϕ_i/‰	386	–38.7	10.9	–41.9	113	0
y_i°	1.9788	1.2102	1.6451	1.3439	1.4037	1.5778

could be measured over a time interval of 25 min. As a reference, IRMS samples were taken for $\delta^{13}C$(DIC) analysis whereas the oxygen concentration was measured with an optode directly inside the Niskin bottles. For the comparison of the oxygen data, the CRDS pO_2 values, which were measured at atmospheric pressure, were converted to the total gas tension of the deep water sample. Since no total gas tension was determined during the experiment, we estimated its value based on the assumption that the water mass was in equilibrium with the atmosphere at a pressure of 1 atm and that its variation is only affected by oxygen depletion.

Assessment

Foci of this work were (*i*) a detailed assessment of the data reduction procedure and (*ii*) a detailed comparison of the field data measured by the CRDS analyzer with data obtained using conventional methods. In the following, the measurements of fCO_2, $\delta^{13}C(CO_2)$, and pO_2 will be assessed separately.

Gas matrix effect on CO_2 measurements

The gas matrix dependent pressure broadening does not only influence the isotope ratio measurements, but also exerts some influence on the measured CO_2 concentration. Since the xCO_2 is determined from peak heights instead of integral absorption, there is a bias for gas matrix compositions different from the reference composition of ambient air. For equilibrated ocean water, the main possible bias stems from the oxygen content. Fig. 3 illustrates the resulting relative CO_2 concentration error as a function of oxygen mole fractions different from air. Data points were calculated based on accurate Voigt line shape parameters for the two probed absorption lines taken from Nakamichi et al. (2006). The nitrogen/argon ratio was kept at its ambient value in all cases. For example, in a typical situation with slight oxygen supersaturation of 2%, the required CO_2 correction is 0.07% and 0.01% for $^{12}CO_2$ and $^{13}CO_2$, respectively. This significant correction sums up to –0.3 ppmv at xCO_2 = 380 ppmv. For field data analysis, the calculated points shown in Fig. 3 were fitted by second-order polynomials and a resulting correction factor, $\xi = [CO_2]_{measured} / [CO_2]_{real}$, has been deduced by including the average natural abundances of the two species $^{12}CO_2$ and $^{13}CO_2$.

$\delta^{13}C(CO_2)$ calibration

In principle, CRDS can be supposed to constitute a "calibration-free" method. It is based on the measurement of light absorption, which is directly linked to the CO_2 concentration via Beer-Lambert's law. Nevertheless, to assure highest accuracy, the instrument was calibrated using a set of reference gas standards. As usual, due to instrumental aging and other effects, this calibration should be repeated on a regular basis. In Fig. 4, $\delta^{13}C(CO_2)$ offsets are shown for pure samples (open circles) of four different compressed air reference gas standards with $\delta^{13}C(CO_2)$ values ranging from –20.2‰ to –3.3‰ and xCO_2 ranging from 350.3 ppmv to 1000.9 ppmv and mixtures of these (filled boxes). All measurements have been performed during the same day. At xCO_2 = 380 ppmv, an offset of 2.8‰ and a dependence of the measured $\delta^{13}C(CO_2)$ value on the total CO_2 content of $\Delta[\delta^{13}C(CO_2)]$ = 0.38‰ per 100 ppmv change in CO_2 could be derived. Repeated measurements on other days yielded similar shaped curves, but variable offsets.

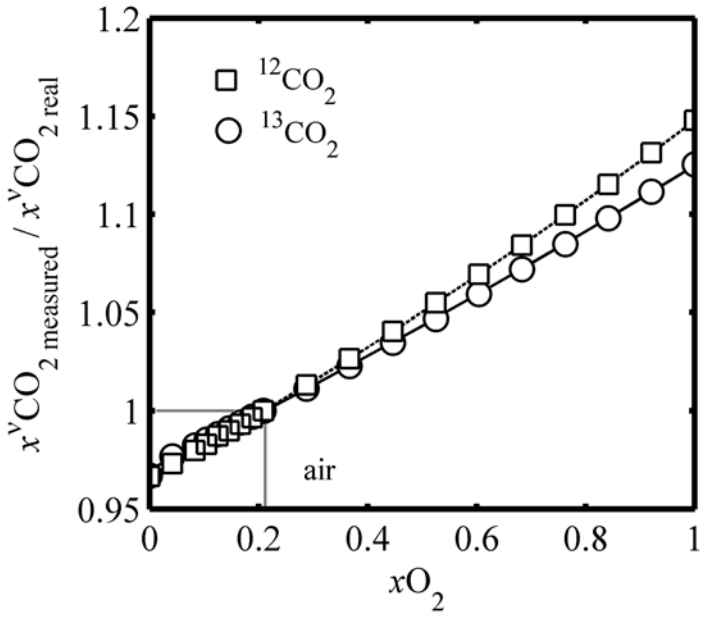

Fig. 3. Gas matrix effect. Influence of oxygen content on the measured CO_2 concentration.

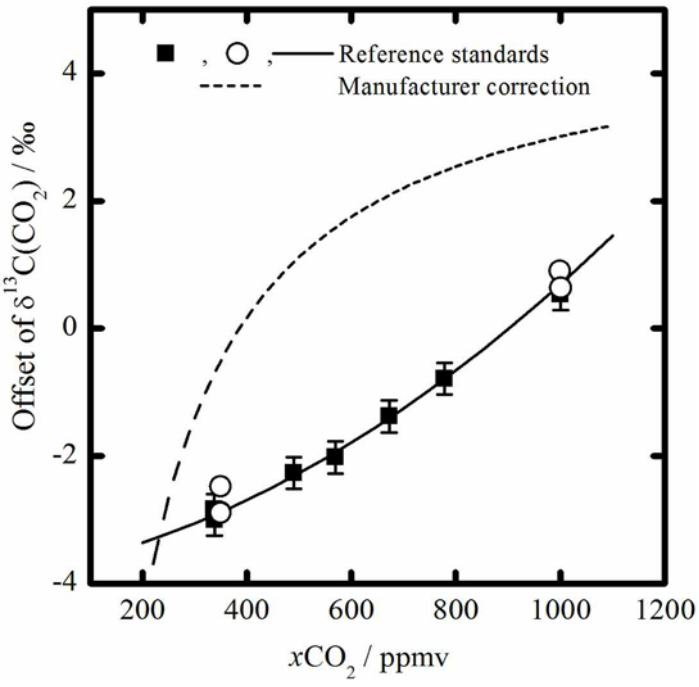

Fig. 4. Dependence of the measured isotope ratio on the amount of CO_2 present in the sample gas mixture. All measurements of the four certified reference samples (open circles) and several gas mixtures (filled boxes) were performed during one day.

The observed strong CO_2 dependence is in obvious contrast with the original manufacturer specification, $\Delta[\delta^{13}C(CO_2)] < 0.03‰$ per 100 ppmv. Consequently, the field data reported in this work were corrected according to the xCO_2 dependence shown in Fig. 4, which had been observed in the laboratory and checked directly before the research cruise in April 2010. Moreover, as outlined in the next section, the instrumental drift of the $\delta^{13}C(CO_2)$ offset was corrected by daily reference gas standard measurements. For the sake of completeness, it should be mentioned that the manufacturer later suggested an alternative correction (dashed curve in Fig. 4) assuming a $[CO_2]^{-1}$ correlation. This correction is based on a reassessment of the original calibration data taking into account identified shortcomings of the calibration protocol. The fact that the proposed xCO_2 dependence does not match our data shows that a frequent check of the instrument's performance is absolutely essential to guarantee its accuracy.

Instrument stability

Since the CRDS analyzer is intended for autonomous, long-term operation on a voluntary observing ship, assessment of the stability of the instrument at sea is an important factor. Relying on the previously found excellent instrument performance on land, the instrument stability for carbon dioxide measurements was expected to be high. Fig. 5A and B illustrate the measured xCO_2 (a) and $\delta^{13}C(CO_2)$ value (b) from daily measurements of the reference gas standard. In case of CO_2, virtually no drift is discernible. With $\Delta(xCO_2) \approx \pm 0.04$ ppmv, the standard deviation of the 5 min moving average is indeed very small. Keeping in mind that no recalibration of the instrument had been performed, these results clearly demonstrate that "calibration-free" measurements of CO_2 content are feasible with this technique.

In contrast, the $\delta^{13}C(CO_2)$ measurements revealed an irregular drift (gray points, lower panel of Fig. 5). Although temperature and humidity conditions during the cruise were highly variable, no significant correlations between the laboratory conditions and the instability of the instrument could be found. Because expected natural oceanic variations of $\delta^{13}C(CO_2)$ are in the ‰ range, a correction of the measured oceanic data with respect to the observed $\delta^{13}C(CO_2)$ instrument drift was necessary. For this propose, a cubic spline interpolation using the averaged standard measurements as base points (open circles) has been fitted to the data. A few of these base points were left out to achieve a smooth curve. Clearly, such a regular recalibration of the instrument's $\delta^{13}C(CO_2)$ readout is essential to meet the precision and accuracy requirements of oceanic measurements.

Underway CO_2 measurements

Reference CO_2 measurements were performed by a second (identical) equilibrator-system equipped with a commonly used NDIR analyzer. The two equilibrator systems were connected to the same flow of seawater and, during atmospheric measurements, the same flow of marine air. In Fig. 6A the fCO_2 values in marine air are shown. The black dots correspond to the CRDS data and the curve to the NDIR data measured five times a day for a few minutes. Moreover, a difference plot of these two datasets is shown in Fig. 6B. The mean offset between the two datasets was found to be $\Delta(fCO_2) = 0.35$ µatm with a standard deviation of 0.29 µatm. This very good agreement of the CRDS and NDIR data is further underlined by the correlation plot shown in Fig. 6C. Correcting with a fixed intercept of 0.35 µatm, the data yield a slope of 1.00003 ± 0.00077, thus indicating a tight agreement of the two datasets within error limits. The offset is well within the stated $\Delta xCO_2 = \pm 0.5$ ppmv accuracy of the calibration of the CRDS instrument.

Corresponding plots for the seawater measurements performed during ANT-XXVI/1 and ANT-XXVI/4 are shown in Fig. 7. Black and gray traces represent data from CRDS/GO system and NDIR/GO system, respectively. Measured fCO_2 values showed strong variations between 150 µatm and 400 µatm. Overall, the observed trends are in close agreement. The difference plot reveals noticeable variations in regions with high variability in fCO_2, e.g., between 50 and 40° south. These variations are most probably due to small differences of the instrumental response times and minor mismatches in the timing of the two datasets. Averaging all data, a systematic offset of $\Delta(fCO_2) = 2.5$ µatm with a standard deviation of 3.0 µatm is

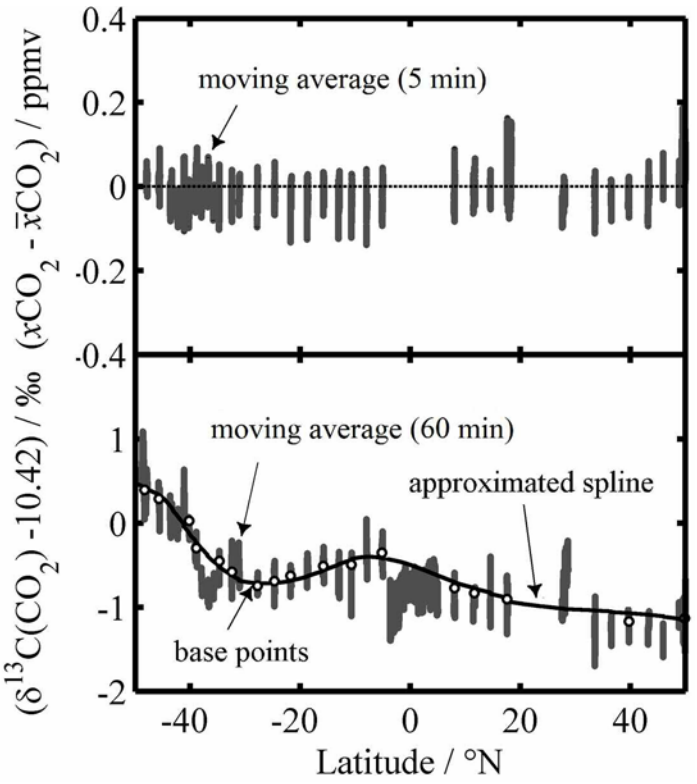

Fig. 5. Instrument stability with respect to xCO_2 (upper panel) and $\delta^{13}C(CO_2)$ (lower panel), both measured during ANT-XXVI/4 cruise. The certified reference standard was accurate to $\delta^{13}C(CO_2) = (10.42 \pm 0.01)‰$ and $xCO_2 = (350 \pm 3)$ ppmv.

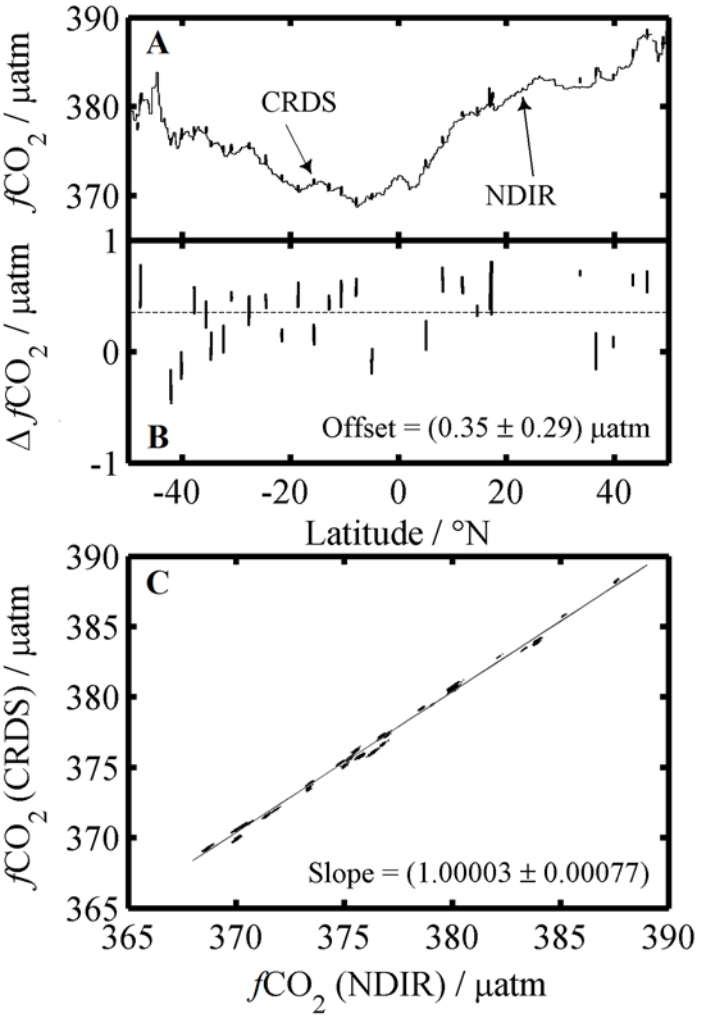

Fig. 6. Comparison of atmospheric fCO_2 measured by CRDS and NDIR during ANT-XXVI/4. A) Original data. B) Difference plot fCO_2(CRDS) – fCO_2(NDIR). C) Correlation plot.

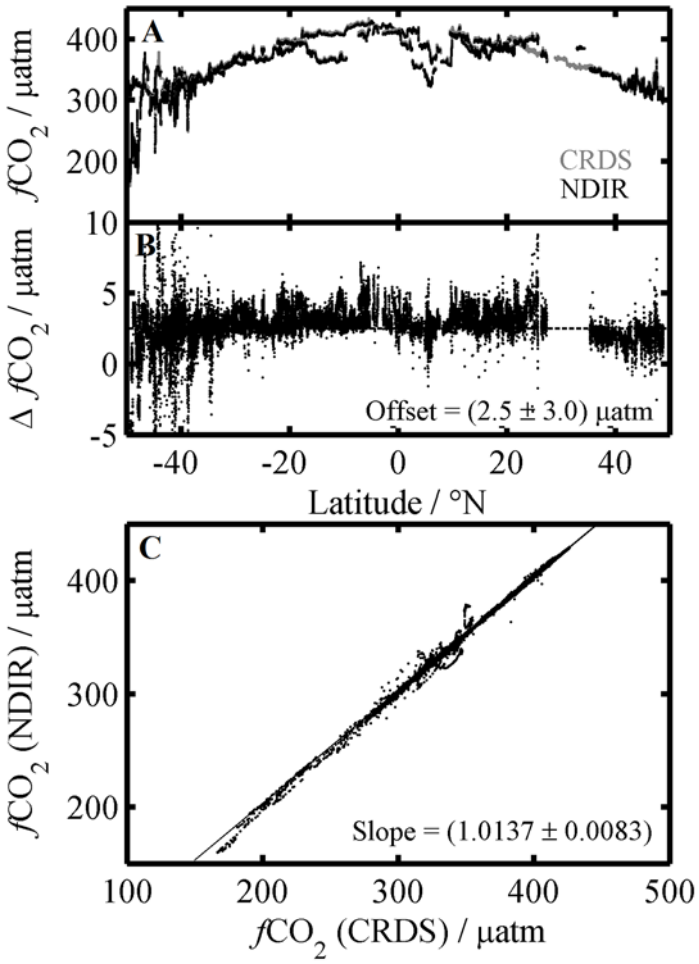

Fig. 7. Comparison of surface ocean fCO_2 measured by CRDS and NDIR during ANT-XXVI/1 and ANT-XXVI/4. A) Original data. B) Combined difference plot fCO_2(CRDS) – fCO_2(NDIR). C) Correlation plot.

evident. In the light of the much smaller offset observed for marine air measurements, this offset has to be attributed to minor differences of the two independent water-air equilibration systems. Note that typical uncertainties of similar equilibration systems have been reported to be on the order of 2 µatm (Pierrot et al. 2009). In particular, in our case, the offset could result from deficient cooling of the Peltier element used in the second drying unit of the NDIR/GO system. This caused a higher water fraction in the sample gas of the NDIR and possibly slightly biased the NDIR measurements as the H_2O channel of the NDIR analyzer was not calibrated. In fact, an even less efficient cooling of the Peltier element can be expected in warmer regions. This would result in measured offsets systematically smaller at higher latitudes than in tropical regions. Another potential source of error could be the accuracy of the seawater temperature measurements at the intake and in the two equilibrators. Any systematic offsets between these will introduce fCO_2 offsets due to the correction procedures for seawater warming. Offsetting the fCO_2 values with a fixed intercept of 2.5 µatm, the correlation plot shown in Fig. 7C yields a slope of 1.0137 ± 0.0083, thus indicating a very good agreement between both datasets.

In summary, a remarkable agreement between the datasets of CRDS and NDIR has been obtained both for marine air and seawater measurements. Actually, the overall accuracy of the method is limited by the performance of the equilibration and drying processes inside the GO-system and not by the accuracy of the CRDS analyzer itself. Taking into account the exceptional drift-free behavior in case of simple CO_2 measurements, the CRDS method is ideally suited for measuring fCO_2. Conventional NDIR systems could be replaced by CRDS instruments resulting in at least comparable accuracy at much reduced calibration effort.

Underway O_2 measurements

The partial pressure of oxygen, pO_2, was determined indirectly by extracting the line broadening parameter of the

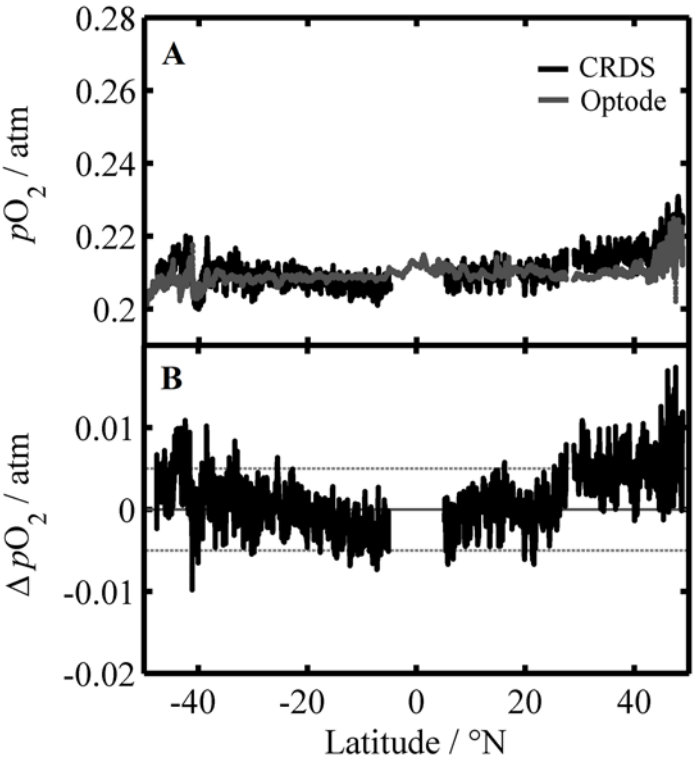

Fig. 8. A) Partial pressure of oxygen measured by CRDS (black curve) and an optode (gray curve) during ANT-XXVI/4. B) Difference plot of the two datasets, the dashed lines indicate an error estimate based on previous calibration data (Friedrichs et al. 2010).

$^{12}CO_2$ absorption line measured by the CRDS analyzer. Fig. 8A illustrates the comparison of the pO_2 data (black curve) with reference measurements using a calibrated optode (gray curve). The CRDS data were continuously averaged over a time interval of 60 min (moving average). Within the scatter of the data, reasonable agreement of the two datasets has been found (see difference plot in Fig. 8B). Note that the precision of the indirect O_2 measurement has been estimated to $\Delta pO_2 = \pm 0.005$ atm in Friedrichs et al. (2010) (dashed lines in Fig. 8B). However, there seems to be a latitudinal trend with too high CRDS values at high latitudes and too low values toward the equator. Although this trend is anticorrelated with measured fCO_2 and water temperature profiles, the reason for it remains unclear. On the one hand, changing amounts of CO_2 content, even on the order of hundreds of ppmv, should not have resulted in detectable line shape effects. On the other hand, the sample cell of the CRDS analyzer was kept at a constant temperature, and therefore, should be independent of ambient conditions. In fact, remaining discrepancies may be partly attributable to the optode measurements as well. As already mentioned in "Materials and procedure," the used optode had been calibrated at a temperature of 25°C and therefore the optode data under colder water conditions at higher latitudes are considered less reliable.

Gas matrix correction

In view of the comparatively small oxygen variations observed during the two cruises, it is difficult to assess the feasibility of a gas matrix correction relying solely on the online CRDS data, i.e., by the data presented in the preceding section. Therefore, two batch experiments with different oxygen concentrations were performed allowing for a more critical check of the applied gas matrix correction. Extracted $\delta^{13}C(CO_2)$ values for batches sampled at different depths are shown in Table 2 with and without the gas matrix correction. For the comparison with reference IRMS samples, the $\delta^{13}C(CO_2)$ CRDS data were converted to $\delta^{13}C(DIC)$. For each batch, the pO_2 measured by the optode and by the CRDS, the isotope ratios measured by IRMS and by CRDS (without and with gas matrix correction, $CRDS_{raw}$ and $CRDS_{O2}$), and corresponding differences between CRDS and IRMS are listed. As can be seen from the low optode pO_2 data, the batches from a depth of 400 m showed a strong undersaturation in oxygen. Due to the limited amount of water available for equilibration, however, the oxygen content in the equilibrated air did not reach these (low) values. Therefore, the gas matrix correction had to be based on the xO_2 measured by the CRDS only. Significantly higher differences between the $CRDS_{raw}$ data and the IRMS data are found at lower oxygen concentrations [see column $\Delta(CRDS_{raw} - IRMS)$]. As expected, inclusion of the gas matrix correction considerably improves the agreement between CRDS and IRMS data [see column $\Delta(CRDS_{O2} - IRMS)$]. The remaining differences can, in part, be attributed to a too short averaging time interval and a systematic offset between the CRDS and IRMS data that will be discussed below. Although this batch experiment did not yield precise enough data to draw final conclusions with respect to the accuracy of the applied gas matrix correction, it again demonstrates its significance and practicability. Overall, the experiment demon-

Table 2. Assessment of the gas matrix correction for batches containing different amounts of dissolved oxygen, see text.

		pO_2/atm		$\delta^{13}C$(DIC)/‰			Δ(CRDS-IRMS)/‰	
Exp.	Depth, m	Optode	CRDS	IRMS	$CRDS_{raw}$	$CRDS_{O2}$	$CRDS_{raw}$	$CRDS_{O2}$
1	400	0.067	0.125	0.2	2.7	0.5	2.5	0.3
1	10	0.198	0.173	1.4	2.9	1.4	1.5	0
2	400	0.067	0.131	0.2	2.8	0.6	2.6	0.4
2	80	0.177	0.167	1.1	2.0	0.6	0.9	–0.5

strates that the oxygen dependent gas matrix correction is necessary. Note that for the underway measurements, in contrast to the batch experiments, the more precise gas matrix corrections relied on simultaneously measured optode oxygen data.

$\delta^{13}C(CO_2)$ field measurements

The measured isotope ratios have been verified by comparison with data from discrete water samples, which were analyzed by IRMS. The CRDS $\delta^{13}C(CO_2)$ field data, which have been converted to $\delta^{13}C(DIC)$ according to the fractionation factors of Zhang et al. (1995) by using Eq. 4, are shown in Fig. 9A (black line). Because no methane concentrations had been measured during the cruise, an approximate methane correction (*see* "Methods and procedure") was based on the assumption that methane dissolved in surface water was in equilibrium with the ambient atmosphere (pCH_4 = 1.8 ppmv). Methane disequilibria in the open ocean are in fact known to be typically small [$\Delta pCH_4 \approx 0.1 - 0.2$ ppmv (Conrad and Seiler 1988)]. Nevertheless, as surface water pCH_4 values of more than 2 µatm have been reported in the shelf areas near the South American coast (Rhee et al. 2009), this imperfect correction may have introduced some bias. Therefore, the presented data south of 45°S as well as north of 45°N should be handled with care. Discrete sample IRMS reference measurements are represented by circles in Fig. 9A and by the cross symbols in the difference plot shown in Fig. 9B. Concerning the overall trend, very good agreement of the CRDS and IRMS data were found. The difference plot reveals a systematic offset of $\Delta[\delta^{13}C(DIC)]$ = 0.33‰ with a standard deviation of 0.20‰. Two outliers have been discarded from the fit because high spatial variations of $\delta^{13}C(DIC)$ and fCO_2 were observed in the respective area at overall low fCO_2. This may have caused additional uncertainties due to possible data matching errors and a less accurate correction of the fCO_2 dependence of the CRDS readout (see Fig. 4). As will be outlined in more detail below, the remaining offset of $\Delta[\delta^{13}C(DIC)]$ = 0.33‰ is well within the expected error limits of the CDRS instrument and the $\delta^{13}C(CO_2)$ to $\delta^{13}C(DIC)$ conversion procedure. The correlation between continuous CRDS data and IRMS samples is shown in Fig. 9C. After fixing the intercept to 0.33‰, the linear correlation yields a slope of 1.00 ± 0.14. Keeping in mind the scatter of the data, these results demonstrate the near one-to-one correlation of both datasets. Summing up, with CRDS, it is possible to obtain online data of isotope ratios at high spatial resolution and good accuracy, thus reducing both the cost and the amount of work needed to collect this type of data.

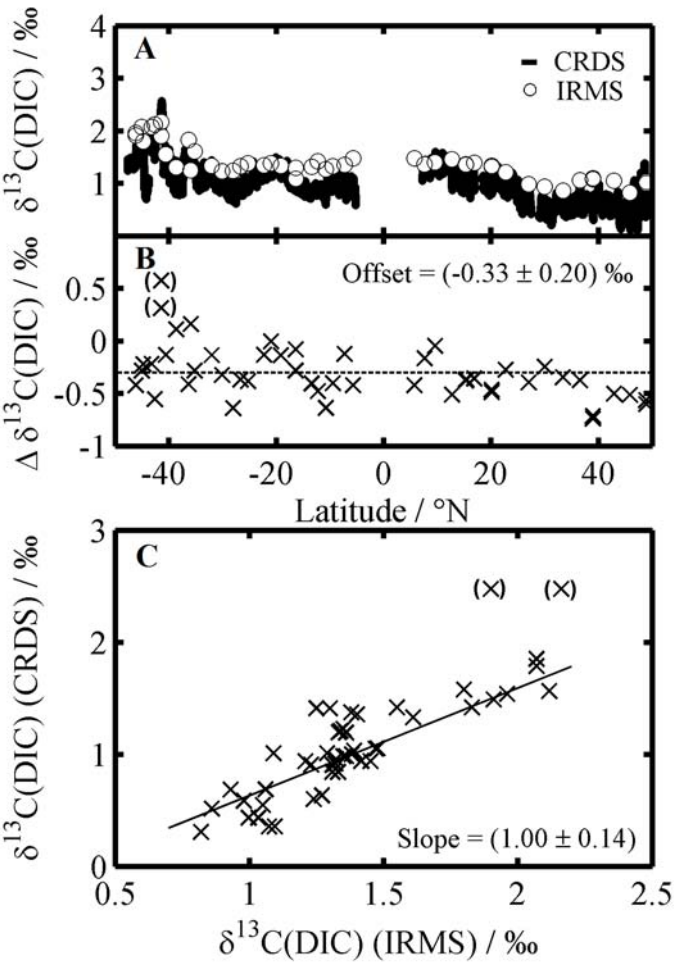

Fig. 9. Comparison of the isotope ratio of carbon dioxide measured by CRDS (converted to $\delta^{13}C(DIC)$) with the $\delta^{13}C(DIC)$ reference measurements obtained by IRMS. Two outliers have been discarded because of high spatial variations of $\delta^{13}C(DIC)$ and fCO_2 at overall low fCO_2 in the respective area. A) Atlantic transect data. B) Difference plot. C) Correlation plot.

Discussion

To use cavity ringdown or cavity-enhanced spectroscopy-based instruments for marine applications on ships, it is important to demonstrate that stable and reliable operation in the field is possible. In this context, the measurements presented in this work served as a critical test. It turned out that the instrument's performance did not appreciable decline during the two cruises, which took place under highly variable climate conditions. Moreover, the CO_2 concentration could be recorded in underway mode with excellent precision and stability. The possibility of high precision measurements of surface water fCO_2 without the need for calibration is a major advantage over conventionally used NDIR systems that need frequent recalibration. For this reason alone, CRDS and CEAS systems hold great potential as next generation trace gas field analyzers.

However, the main purpose of this study was to establish continuous $\delta^{13}C(DIC)$ measurement capabilities in surface water to add an additional parameter to better constrain environmental carbon fluxes. Here, to achieve the required accuracy, the system had to be calibrated on a regular basis. Based on our experience, a full calibration including the $\delta^{13}C(CO_2)$ readout dependence on total CO_2 should be performed at least

once before and after each cruise. Additionally, to overcome drift components on shorter timescales (see Fig. 5), it was necessary to measure one reference gas for 3 h at least once a day. To achieve a precision better than 0.1‰, switching between sample and reference gas standard every 2 min has been proposed (Rella 2011). An even further improved performance of CRDS analyzers with respect to precision and averaging time can be expected in the near future with ever optimized instruments.

A specific issue of our instrument resulting from measuring center-of-line absorption instead of integral absorption is that a gas matrix correction is required both for fCO_2 and $\delta^{13}C(CO_2)$. For marine application, required corrections are mainly caused by varying O_2 content and are small for fCO_2 (typically a few tenth of ppmv) and significant for $\delta^{13}C(CO_2)$ (e.g., –0.2‰ for 104% oxygen saturation at fCO_2 = 380 µatm). As can be concluded from the oxygen measurements presented in Fig. 8 and the batch experiment summarized in Table 2, measuring pO_2 from the line-width data reported by the instrument itself is feasible at an accuracy in pO_2 of approximately 0.005 atm. For $\delta^{13}C(CO_2)$, the attainable precision is approximately 0.2‰. If better precision is needed, a calibrated optode needs to be run in parallel.

Another element of uncertainty when reporting $\delta^{13}C(DIC)$ instead of equilibrium $\delta^{13}C(CO_2)$ is linked to the isotope fractionation factors between gaseous CO_2 and DIC, ε_{DIC-CO_2}. In contrast to many atmospheric applications, the correlation of marine CO_2 parameters requires the knowledge of the isotopic composition of DIC instead of the isotopic composition of the CO_2 itself. Important examples are the correlation of surface water DIC with $\delta^{13}C(DIC)$ using Keeling plots (Köhler et al. 2006; Yakir and Sternberg 2000) or the quantification of the oceanic Suess effect by comparing current $\delta^{13}C(DIC)$ data measured by CRDS with literature data measured by IRMS (Körtzinger et al. 2003). The latter requires a higher precision than achieved in this work, hence it relies on future CRDS analyzers with improved performance. Of course, the $\delta^{13}C(CO_2)$ to $\delta^{13}C(DIC)$ conversion is not a specific problem of CRDS, but this application calls for a redetermination of fractionation factor over a suitable temperature, salinity, and pH range because it currently limits the accuracy of our reported $\delta^{13}C(DIC)$ data.

Several studies dealt with the fractionation factors of the carbonate system in freshwater [e.g., Mook (1986) and Zhang et al. (1995)], but only two studies are available for the fractionation in seawater (Inoue and Sugimura 1985; Zhang et al. 1995). Note that fractionation factors for freshwater are hardly comparable with those in seawater since the equilibrium constants are salinity dependent. Moreover, the high concentrations of Mg^{2+} and Na^+ affect the speciation within the carbonate system as well as the isotopic composition of DIC by the presence of sodium and magnesium complexes of bicarbonate and carbonate (Thode et al. 1965; Garrels et al. 1961).

During the present cruise salinity values varied from 33.5 < S < 37.5 such that an accurate $\delta^{13}C(CO_2)$ to $\delta^{13}C(DIC)$ conversion needs to include the salinity dependence of the fractionation factors. Inoue and Sugimura (1985) determined the ε_{DIC-CO_2} fractionation factor at a salinity of S = 34.75 and pH = 8.3 at five different temperatures. Also Zhang et al. (1995) reported values for different temperatures and pH values, but unfortunately, the salinity of the used seawater, which was collected in the North Pacific, was not given. In Fig. 10A, published temperature dependencies of the fractionation factors ε_{DIC-CO_2} are presented. The different curves were calculated for a typical seawater speciation of CO_2 : HCO_3^- : CO_3^{2-} = 0.5% : 86.5% : 13%. Additionally, the original seawater data of Inoue and Sugimura (1985) are shown as cross symbols. In Fig. 10B, the calculated ε_{DIC-CO_2} values are shown for our cruise data. The overall trend with lower ε_{DIC-CO_2} fractionation factors near the equator largely reflects the varying water temperature conditions. Unfortunately, the presented datasets are not consistent. For example, although Zhang et al. (1995) reported a significant salinity dependence, their seawater data are more or less consistent with the freshwater data of Mook (1986). Given

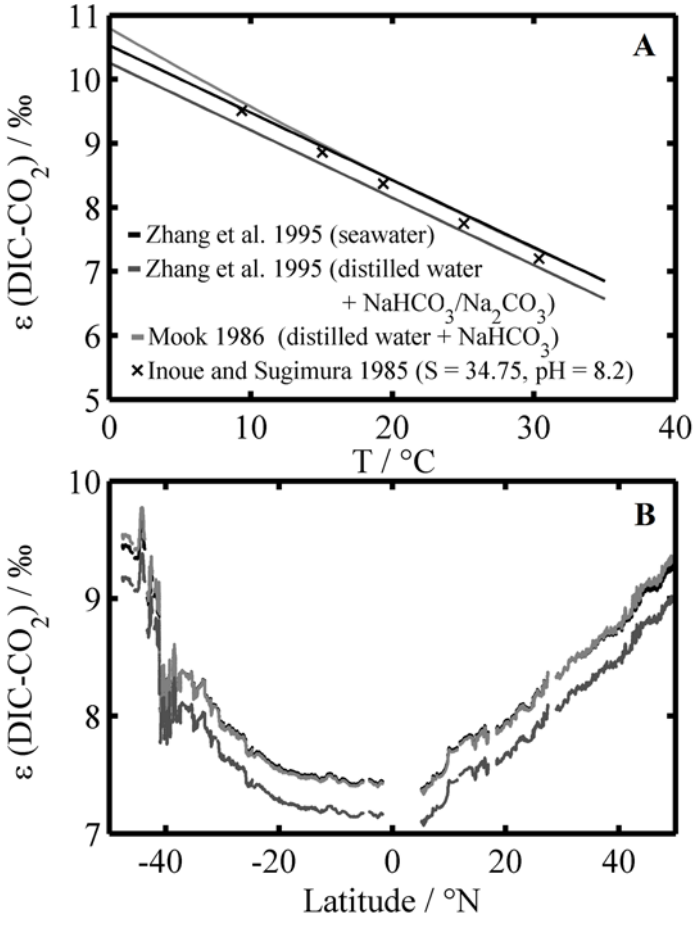

Fig. 10. Fractionation factor $\varepsilon_{DIC-CO2}$. A) Temperature dependence of the fractionation factor, calculated for a typical seawater speciation of CO_2 : HCO_3^- : CO_3^{2-} = 0.5% : 86.5% : 13%. B) Calculated $\varepsilon_{DIC-CO2}$ values for the cruise data (with varying temperature).

this inconsistency, we estimate the potential systematic uncertainty of our reported $\delta^{13}C(DIC)$ values to be up to ± 0.3‰ based on the temperature dependent DIC-CO_2 conversion alone.

In Fig. 11, a similar analysis is shown for the carbonate system speciation dependence, which was calculated for a fixed temperature of 25°C using TA = $f(S)$ as the second CO_2 system parameter (see "Materials and Procedure"). Next to the already discussed systematic offsets of the different ε_{DIC-CO_2} datasets, additional inconsistencies arise from the irregular behavior of ε_{DIC-CO_2} with respect to the speciation. Note that the trends of the ε_{DIC-CO_2} conversion outlined in Fig. 11 even show a reversed behavior depending on the literature source used. We estimate an additional, speciation dependent uncertainty on the order of $\Delta[\delta^{13}C(DIC)] \approx \pm 0.05$‰.

Taking the mentioned ε_{DIC-CO_2} conversion errors together, the resulting uncertainty of $\Delta[\delta^{13}C(DIC)] \approx \pm 0.35$‰ could account for the remaining difference of 0.33‰ observed between IRMS and CRDS $\delta^{13}C(DIC)$ data as outlined in Fig. 9. An additional uncertainty arises from the calibration of the instrument (≤0.3‰). Hence, it can be stated that the IRMS and CRDS data are, in fact, consistent within current error limits. Obviously, improved calibration of the instrument as well as more accurate ε_{DIC-CO_2} values are needed to reduce these systematic errors in future measurements. In contrast, relative trends of $\delta^{13}C(CO_2)$ are reliably resolved as demonstrated by the near one-to-one correlation of IRMS and CRDS data shown in Fig. 9C.

Finally, full cruise data are shown in Fig. 12. These data represent the first continuous and simultaneous measurements of fCO_2 and $\delta^{13}C(CO_2)$ in surface ocean waters along an ocean transect. Preliminary analysis of subsets of these data revealed anti-correlated behavior of fCO_2 and $\delta^{13}C(CO_2)$. This is to be

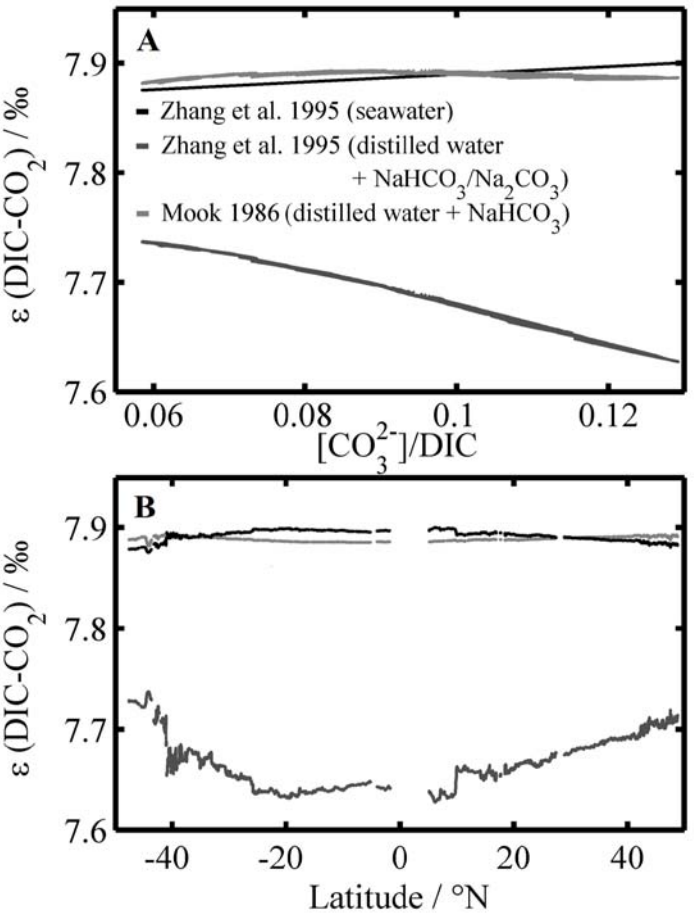

Fig. 11. Fractionation factor $\varepsilon_{DIC-CO2}$. A) Speciation dependence of the fractionation factor, calculated for a temperature of 25°C and the speciation as calculated from fCO_2 and TA. B) Calculated $\varepsilon_{DIC-CO2}$ values for the cruise data (with varying speciation).

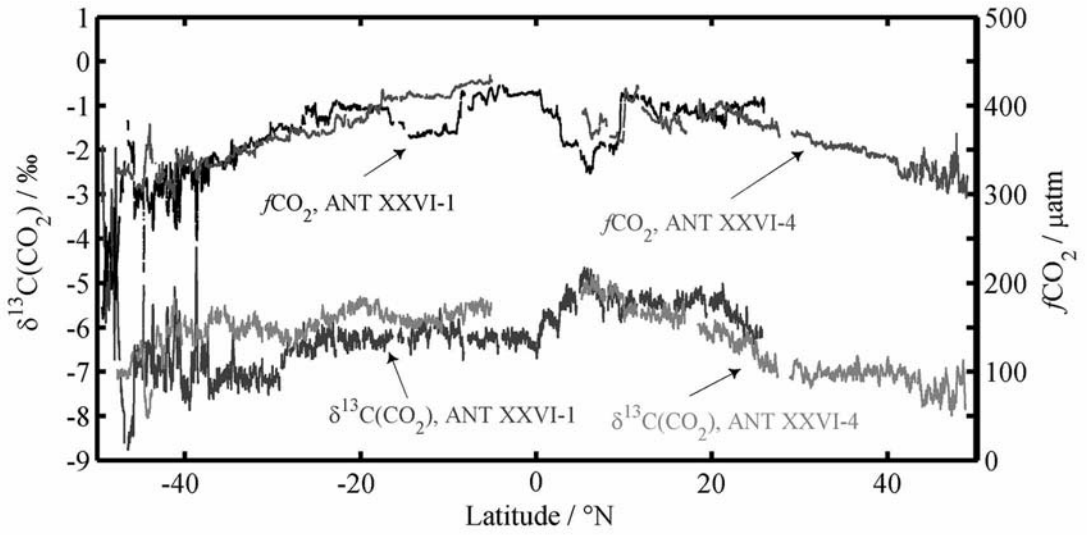

Fig. 12. Surface ocean fCO_2 and $\delta^{13}C(CO_2)$ measured during ANT-XXVI/1and ANT-XXVI/4.

expected in ocean regions where primary production causes lower DIC concentrations. However, a detailed analysis should await the accumulation of more data and should be based on an improved data conversion procedure as outlined above. Especially, measurements need to be more properly corrected for the mentioned CH_4 cross-sensitivity. Currently, a manufacturer upgrade of the instrument is underway that will allow to simultaneously measure and correct for CH_4.

Despite these remaining issues, our field measurements clearly demonstrate that CRDS is capable of highly accurate and "calibration-free" monitoring of CO_2 concentrations. Already the first transect data revealed that the isotope ratio of dissolved inorganic carbon in surface ocean water can be determined with satisfying precision and accuracy. The easy handling, high precision, and robustness of the instrument is superior to other related techniques. Up to now, daily measurements of reference gas standards are still necessary to correct for $\delta^{13}C(CO_2)$ baseline drifts. Also the instrument's response to changing CO_2 concentrations needs to be checked regularly. For seawater measurements, changes in the gas matrix of the equilibrated gases have to be properly taken into account as well.

References

Bass, A. M., M. I. Bird, N. C. Munksgaard, and C. M. Wurster. 2012. ISO-CADICA: Isotopic – continuous, automated dissolved inorganic carbon analyser. Rapid Commun. Mass Spectrom. 26:639-644 [doi:10.1002/rcm.6143].

Bergamaschi, P., M. Schupp, and G. W. Harris. 1994. High-precision direct measurements of $^{13}CH_4/^{12}CH_4$ and $^{12}CH_3D/^{12}CH_4$ ratios in atmospheric methane sources by means of a long-path tunable diode laser absorption spectrometer. Appl. Opt. 33:7704-7716 [doi:10.1364/AO.33.007704].

Conrad, R., and W. Seiler. 1988. Methane and hydrogen in seawater (Atlantic Ocean). Deep-Sea Res. 35:1903-1917 [doi:10.1016/01980149(88)901161].

Crosson, E. R., and others. 2002. Stable isotope ratios using cavity ringdown spectroscopy: Determination of $^{13}C/^{12}C$ for carbon dioxide in human breath. Anal. Chem. 74:2003-2007 [doi:10.1021/ac025511d].

de Groot, P. A. [ed.]. 2004. Handbook of stable isotope analytical techniques. Elsevier.

Dickson, A. G., and F. J. Millero. 1987. A comparison of the equilibrium constants for the dissociation of carbonic acid in seawater media. Deep-Sea Res. 34:1733-1743 [doi:10.1016/01980149(87)900215].

———, C. L. Sabine, and J. R. Christian [eds.]. 2007. Guide to best practices for ocean CO_2 measurements. PICES Special Publication 3.

Friedrichs, G. 2008. Sensitive absorption methods for quantitative gas phase kinetic measurements. Part 2: Cavity ringdown spectroscopy. Z. Phys. Chem. 222:31-61 [doi:10.1524/zpch.2008.222.1.31].

———, J. Bock, F. Temps, P. Fietzek, A. Körtzinger, and D. W. R. Wallace. 2010. Toward continuous monitoring of seawater $^{13}CO_2/^{12}CO_2$ isotope ratio and pCO_2: Performance of cavity ringdown spectroscopy and gas matrix effects. Limnol. Oceanogr. Methods 8:523-551 [doi:10.4319/lom.2010.8.539].

Galatry, L. 1961. Simultaneous effect of Doppler and foreign gas broadening on spectral lines. Phys. Rev. 122:1218-1223 [doi:10.1103/PhysRev.122.1218].

Garrels, R. M., M. E. Thompson, and R. Siever. 1961. Control of carbonate solubility by carbonate complexes. Am. J. Sci. 259:24-45 [doi:10.2475/ajs.259.1.24].

Ghosh, P., and W. A. Brand. 2003. Stable isotope ratio mass spectrometry in global climate change research. Int. J. Mass Spectrom. 228:1-33 [doi:10.1016/S13873806(03)002896].

Graham, W. M., R. H. Condon, R. H. Carmichael, I. D'Ambra, H. K. Patterson, L. J. Linn, and F. J. Hernandez Jr. 2010. Oil carbon entered the coastal planktonic food web during the Deepwater Horizon oil spill. Environ. Res. Lett. 5:045301/1–6 [doi:10.1088/1748-9326/5/4/045301].

Gupta, P., D. Noone, J. Galewsky, C. Sweeney, and B. H.Vaughn. 2009. Demonstration of high-precision continuous measurements of water vapor isotopologues in laboratory and remote field deployments using wavelength-scanned cavity ring-down spectroscopy (WS-CRDS) technology. Rapid Commun. Mass Spectrom. 23:2534-2542 [doi:10.1002/rcm.4100].

Haisch, M., P. Hering, P. Schadewaldt, H. Brösicke, B. Braden, S. Koletzko, and C. Steffen. 1994. Biomedical application of an isotope selective nondispersive infrared spectrometer for $^{13}CO_2$ and $^{12}CO_2$ concentration measurements in breath samples. Isot. Environ. Health Stud. 30:253-257 [doi:10.1080/00211919408046741].

Inoue, H., and Y. Sugimura. 1985. Carbon isotopic fractionation during the CO_2 exchange process between air and sea water under equilibrium and kinetic conditions. Geochim. Cosmochim. Acta 49:2453-2460 [doi:10.1016/00167037(85)902455].

Jäger, F., G. Wagner, H. A. J. Meijer, and E. R. T. Kerstel. 2005. Measuring $\delta^{13}C$ of atmospheric air with non-dispersive infrared spectroscopy. Isot. Environ. Health Stud. 41:373-378 [doi:10.1080/10256010500384275].

Jost, H.-J., A. Castrillo, and H. W. Wilson. 2006. Simultaneous $^{13}C/^{12}C$ and $^{18}O/^{16}O$ isotope ratio measurements on CO_2 based on off-axis integrated cavity output spectroscopy. Isot. Environ. Health Stud. 42:37-45 [doi:10.1080/10256010500503163].

Keeling, C. D., S. C. Piper, R. B. Bacastow, M. Wahlen, T. P. Whorf, M. Heimann, and H. A. Meijer. 2005. Atmospheric CO_2 and $^{13}CO_2$ exchange with the terrestrial biosphere and oceans from 1978 to 2000: Observations and carbon cycle implications. Ecol. Stud. 177:83-113 [doi:10.1007/038727048855].

Kerstel, E., and L. Gianfrani. 2008. Advances in laser-based iso-

tope ratio measurements: selected applications. Appl. Phys. B 92:439-449 [doi:10.1007/s003400083128x].

Köhler, P., H. Fischer, J. Schmitt, and G. Munhoven. 2006. On the application and interpretation of Keeling plots in paleo climate research—deciphering $\delta^{13}C$ of atmospheric CO_2 measured in ice cores. Biogeosciences 3:539-556 [doi:10.5194/bg35392006].

Körtzinger, A., and others. 2000. The international at-sea intercomparison of fCO_2 systems during the R/V Meteor Cruise 36/1 in the North Atlantic Ocean. Mar. Chem. 72:171-192 [doi:10.1016/S0304-4203(00)00080-3].

———, P. D. Quay, and R. E. Sonnerup. 2003. Relationship between anthropogenic CO_2 and the ^{13}C Suess effect in the North Atlantic Ocean. Global Biogeochem. Cycles 17:1-20 [doi:10.1029/2001GB001427].

Krevor, S., J.-C. Perrin, A. Esposito, C. Rella, and S. Benson. 2010. Rapid detection and characterization of surface CO_2 leakage through the real-time measurement of $\delta^{13}C$ signatures in CO_2 flux from the ground. Int. J. Greenhouse Gas Control 4:811-815 [doi:10.1016/j.ijggc.2010.05.002].

Mazurenka, M., A. J. Orr-Ewing, R. Peverall, and G. A. D. Ritchie. 2005. Cavity ringdown and cavity enhanced spectroscopy using diode lasers. Annu. Rep. Prog. Chem. 101:100-142 [doi:10.1039/b408909j].

McAlexander, I., G. H. Rau, J. Liem, T. Owano, R. Fellers, D. Baer, and M. Gupta. 2011. Deployment of a carbon isotope ratiometer for the monitoring of CO_2 sequestration leakage. Anal. Chem. 83:6223-6229 [doi:10.1021/ac2007834].

Mehrbach, C., C. Culberson, J. Hawley, and R. Pytkowicz. 1973. Measurement of the apparent dissociation constants of carbonic acid in seawater at atmospheric pressure. Limnol. Oceanogr. 18:897-907 [doi:10.4319/lo.1973.18.6.0897].

Mikhailenko, S. N., K. A. Keppler, G. Mellau, S. Klee, B. P.Winnewisser, M. Winnewisser, and V. G. Tyuterev. 2008. Water vapor absorption line intensities in the 1900- 6600 cm-1 region. J. Quant. Spectrosc. Radiat. Transfer. 109:2687-2696 [doi:10.1016/j.jqsrt.2008.07.006].

Mohn, J., R. A. Werner, B. Buchmann, and L. Emmenegger. 2007. High-precision $\delta^{13}CO_2$ analysis by FTIR spectroscopy using a novel calibration strategy. J. Mol. Struct. 834836:95-101 [doi:10.1016/j.molstruc.2006.09.024].

Mook, W. 1986. ^{13}C in atmospheric CO_2. Neth. J. Sea Res. 20:211-223 [doi:10.1016/00777579(86)900438].

Murnick, D. E., and B. J. Peer. 1994. Laser-based analysis of carbon isotope ratios. Science 263:945-947 [doi:10.1126/science.8310291].

Nakamichi, S., and others. 2006. Buffer-gas pressure broadening for the (3 0^0 1)III ← (0 0 0) band of CO_2 measured with continuous-wave cavity ringdown spectroscopy. Phys. Chem. Chem. Phys. 8:364-368 [doi:10.1039/b511772k].

Perevalov, B. V., and others. 2008a. Global modeling of $^{13}C^{16}O_2$ absolute line intensities from CW-CRDS and FTS measurements in the 1.6 and 2.0 μm regions. J. Quant. Spectrosc. Radiat. Transfer 109:2009-2026 [doi:10.1016/j.jqsrt.2008.02.008].

———, A. Campargue, B. Gao, S. Kassi, S. A. Tashkun, and V. I. Perevalov. 2008b. New CW-CRDS measurements and global modeling $^{12}C^{16}O_2$ absolute line intensities in the 1.6 μm region. J. Mol. Spectrosc. Radiat. Transfer 252:190-197 [doi:10.1016/j.jms.2008.08.006].

Pierrot, D., and others. 2009. Recommendations for autonomous underway pCO_2 measuring systems and data-reduction routines. Deep-Sea Res. II 56:512-522 [doi:10.1016/j.dsr2.2008.12.005].

Quay, P. D., R. Sonnerup, T. Westby, J. Stutsman, and A. McNichol. 2003. Changes in the $^{13}C/^{12}C$ of dissolved inorganic carbon in the ocean as a tracer of anthropogenic CO_2 uptake. Global Biogeochem. Cycles 17:1-20 [doi:10.1029/2001GB001817].

———, R. Sonnerup, J. Stutsman, J. Maurer, A. Körtzinger, X. A. Padin, and C. Robinson. 2007. Anthropogenic CO_2 accumulation rates in the North Atlantic Ocean from changes in the $^{13}C/^{12}C$ of dissolved inorganic carbon. Global Biogeochem. Cycles 21:1-15 [doi:10.1029/2006GB002761].

———, J. Stutsman, R. A. Feely, and L.W. Juranek. 2009. Net community production rates across the subtropical and equatorial Pacific Ocean estimated from air-sea $\delta^{13}C$ disequilibrium. Global Biogeochem. Cycles 23:1-15 [doi:10.1029/2008GB003193].

Rella, C. 2011. Reduced drift, high accuracy stable carbon isotope ratio measurements using a reference gas with the Picarro $\delta^{13}CO_2$ G2101-i gas analyzer. <http://www.picarro.com/assets/docs/White_Paper_G2101-i_Drift_Reduction.pdf>.

Rhee, T. S., A. J. Kettle, and M. O. Andreae. 2009. Methane and nitrous oxide emissions from the ocean: A reassessment using basin-wide observations in the Atlantic. J. Geophys. Res. 114:D12304.

Romanini, D., A. A. Kachanov, N. Sadeghi, and F. Stoeckel. 1997. CW cavity ring-down spectroscopy. Chem. Phys. Lett. 264:316-322 [doi:10.1016/S00092614(96)013516].

Sabine, C. L., and others. 2004. The oceanic sink for anthropogenic CO_2. Science 305:367-371 [doi:10.1126/science.1097403].

Stramma, L., G. C. Johnson, J. Sprintall, and V. Mohrholz. 2008. Expanding oxygen-minimum zones in the tropical oceans. Science 320:655-658.

Takahashi, T., S. C. Sutherland, and A. Kozyr. 2011. Global ocean surface water partial pressure of CO_2 database: measurements performed during 1957-2010 (Version 2010). ORNL/CDIAC-159, NDP-088(V2010). Carbon Dioxide Information Analysis Center, Oak Ridge National Laboratory, U.S. Department of Energy, Oak Ridge, Tennessee [doi:10.3334/CDIAC/otg.ndp088(V2010)].

Thode, H. G., M. Shima, C. E. Rees, and K. V. Krishnamurty. 1965. Carbon-13 isotope effects in systems containing carbon dioxide, bicarbonate, carbonate, and metal ions. Can. J. Chem. 43:582-595 [doi:10.1139/v65076].

van Heuven, S., D. Pierrot, E. Lewis, and D. Wallace. 2009. MATLAB program developed for CO_2 system calculations. ORNL/CDIAC105b.

Wahl, E. H., and others. 2006. Applications of cavity ring-down spectroscopy to high precision isotope ratio measurement of $^{13}C/^{12}C$ in carbon dioxide. Isot. Environ. Health Stud. 42:21-35 [doi:10.1080/10256010500502934].

Yakir, D., and L. d. S. L. Sternberg. 2000. The use of stable isotopes to study ecosystem gas exchange. Oecologia 123:297-311 [doi:10.1007/s004420051016].

Zhang, J., P. D. Quay, and D. O. Wilbur. 1995. Carbon isotope fractionation during gas-water exchange and dissolution of CO_2. Geochim. Cosmochim. Acta 59:107-14 [doi:10.1016/00167037(95)91550D].

Submitted 21 December 2011
Revised 5 June 2012
Accepted 19 June 2012